Applicability of the mean field theory to the Ising and Néel models of magnetism

Joe Blake, Will Bolton, and Michael Negus

(Dated: 23 December 2022)

Approximations for the quantities related to magnetic materials, including magnetisation and magnetic susceptibility, were assessed for their accuracy using computer simulation by applying the mean field theory to the Ising and Néel models. These included: measuring the magnetisation against magnetic field at constant temperatures, calculating regions where the mean field theory most accurately predicts the magnetisation at different magnetic fields and temperatures, determining how well the magnetic susceptibility is predicted in the Néel model and the time for the magnetisation to reverse below the Curie temperature in the Ising model.

I. INTRODUCTION

Having reliable models for the behaviour of magnetic materials has become essential for many applications, for example, magnetoresistant sensors are used in the read heads of hard disk drives[1]. The Ising and Néel models describe ferromagnetism and antiferromagnetism at the atomic scale by considering quantum mechanical exchange interactions. These exchanges are difficult to measure due to their microscopic scale and huge number of possible states making analytical and numerical solutions impractical to study and therefore a studying simulations is required. Mean field theory can be applied to the Ising and Néel models to make approximations to values such as magnetisation, in terms of quantities that can be measured macroscopically, like temperature and applied magnetic field. This paper aims to assess how well mean field theory predicts some of these quantities. To do this, simulations of the Ising and Néel models were employed, which allow for direct measurement of quantities such as magnetisation which is not possible for experiments.

II. THE ISING MODEL

A. Preliminaries

For the sake of brevity, we begin our derivation of the theory[2] starting from the Heisenberg Hamiltonian[3]. The Heisenberg Hamiltonian is defined as

$$\mathcal{H} = -\frac{1}{2}\sum_i \sum_{j\neq i} \mathscr{J}_{ij}\mathbf{S}_i \cdot \mathbf{S}_j - \mu \sum_i \mathbf{H}_i \cdot \mathbf{S}_i, \tag{1}$$

and it equates the total energy of a system of spins. When adjacent atomic spins are aligned, the total energy is lowered as two atoms with parallel spins cannot be in proximity with each other according to the Pauli exclusion principle. Here, $\mathscr{J}_{ij}$ is the interaction energy originating from the electrostatic potential between spin sites i and j. Although the ising model can take negative values, it is currently assumed that $\mathscr{J}_{ij}$ is positive, as the negative case is addressed with the Néel Model. $\mathbf{S}_i$ is the component of spin at the site (potentially $\mathbf{J}$, $\mathbf{L}$ or $\mathbf{S}$), $\mathbf{H}_i$ is the external magnetic field at site i, and μ is the atomic magnetic moment of the site particle. This Hamiltonian can be simplified by assuming $\mathscr{J}_{ij} = \mathscr{J}$ when spins $\mathbf{S}_i$ and $\mathbf{S}_j$ are neighbours and $\mathscr{J}_{ij} = 0$ otherwise, and assuming that the external magnetic field is uniform across the sample. This leads to a simplified version;

$$\mathcal{H} = \mathscr{J}\sum_{\langle i,j\rangle} \mathbf{S}_i \cdot \mathbf{S}_j - \mu \sum_i \mathbf{H} \cdot \mathbf{S}_i, \tag{2}$$

where $\langle i, j\rangle$ indicates non-repeating pairs of nearest neighbours.

B. Magnetisation

An approximation to the effective magnetic field acting on a magnetic moment is the Weiss molecular field

$$\mathbf{H}_{\text{eff}} = \mathbf{H} + \lambda_I \mathbf{M}, \tag{3}$$

where $\mathbf{H}_{\text{eff}}$ is the effective field, $\mathbf{H}$ is the real magnetic field at the atom, $\mathbf{M}$ is the magnetisation. The dimensionless quantity λ_I is given by

$$\lambda_I = \frac{2\sum_{j\neq i} \mathscr{J}_{ij}}{N\mu_0 g^2 \mu_B^2}, \tag{4}$$

where N is the number of spins per unit volume, μ_0 is the permeability of free space, g is the Landé g-factor and μ_B is the Bohr magneton[2] and the sum is over the nearest neighbours. In order to determine the magnetisation of a ferromagnet, we consider the case where the magnetic moment of each atom is due to a single electron spin (so $g = 2$), and mean field theory gives

$$M = N\mu_B \tanh\Big(\frac{\mu_B \mu_0 H_{\text{eff}}}{k_B T}\Big), \tag{5}$$

where k_B is the Boltzmann constant and T is temperature[2]. Substituting equation (3) into equation (5) gives the implicit equation for the magnetisation

$$\frac{M}{N\mu_B} = \tanh\left(\frac{\mu_B\mu_0 H + 4\mathscr{J}\frac{M}{N\mu_B}}{k_B T}\right). \tag{6}$$

C. Expected value of each spin

The partition function of the system of atoms is given by[4]

$$Z = \sum_i \exp\Big(\frac{\mathcal{E}_i}{k_B T}\Big) \tag{7}$$

Where $\mathcal{E}_i$ is the energy of each state. The only possible values of spin for each atom are ± 1 so Z can be factorised into N factors where N is the total number of states with

$$Z = (Z_1)^N,\ Z_1 = \sum_{i=\pm 1} \exp\Big(\frac{\mathcal{E}_i}{k_B T}\Big) \tag{8}$$

For a non interacting system we can write $\mathcal{E}_\pm = \pm\mathcal{E}$ giving[4]

$$Z_1 = 2\cosh\Big(\frac{\mathcal{E}}{k_B T}\Big), \tag{9}$$

The probabilities for the spin of each atom are given by

$$P_\pm = \frac{\exp\left(\frac{\pm\mathcal{E}}{k_B T}\right)}{Z_1}. \tag{10}$$

This gives the expected value of a single spin,

$$\langle S_i\rangle = \tanh\Big(\frac{\mathcal{E}}{k_B T}\Big). \tag{11}$$

When dealing with interacting spins the problem becomes much more difficult; the large number of possible states of the system renders numerical solutions unfeasible. Using the mean field approximation we find that at high temperatures the system favours a state where $M = 0$ but at low temperatures the system prefers a magnetic phase and the spins will tend to spontaneously align along the two preferred values of $M = \pm M_0$, where $M_0 = N\mu$ is the saturation magnetisation, obtained by aligning all of the N spins of magnetic permeability μ. This is because the exchange effect begins to outweigh the diminishing thermal effects.[4,5]

D. Curie temperature

The Curie temperature is defined to be[2]

$$T_C = \lambda_I C, \tag{12}$$

where C is the Curie constant, given by

$$C = \frac{N\mu_0\mu_B^2}{k_b}. \tag{13}$$

In the case where $g = 2$, this gives

$$T_C = 2\mathscr{J}/k_B \tag{14}$$

In the absence of an external magnetic field, the Curie temperature is the highest temperature the Weiss model predicts for materials to exhibit ferromagnetic behaviour. For $T < T_C$, the exchange effect dominates and the spins spontaneously align. For $T \gg T_C$, thermal effects dominate over the exchange interaction and the spins tend to align less. In this regime we can use the $\tanh x \approx x$ approximation to derive a relationship between magnetic susceptibility and temperature:

$$\chi = \frac{C}{T - T_C}, \tag{15}$$

known as the Curie-Weiss Law[2].

III. THE NÉEL MODEL

We return to the Heisenberg Hamiltonian EQ.(2), and investigate the case: $\mathscr{J}_{ij} < 0$. In this case antiparallel alignment is energetically preferential in the absence of an external magnetic field. This leads to an arrangement where up and down spins alternate, and no macroscopic magnetisation occurs without external magnetic field.

The Néel Model separates these alternating spins into two sublattices A and B, such that the mean magnetic moment on each site of A is antiparallel to that of B. This often means that every nearest neighbour of a member of B is a member of A.

In the Néel Model, we replace the Weiss Field EQ.(3) with sublattice equations

$$\mathbf{B}^A_{\text{eff}} = \mu_0(\mathbf{H} - \lambda_N\mathbf{M}_B) \quad \text{and} \quad \mathbf{B}^B_{\text{eff}} = \mu_0(\mathbf{H} - \lambda_N\mathbf{M}_A), \tag{16}$$

where $\mathbf{M}_A$ and $\mathbf{M}_B$ are the contributions to total magnetisation from sublattices A and B respectively. These are derived from (2) by neglecting all interactions further than the nearest neighbour and assuming every nearest neighbour of a member of B is a member of A.

Further derivation leads to

$$\lambda_N = -\frac{4\sum_{j\neq i}\mathscr{J}_{ij}}{N\mu_0 g^2\mu_B^2} = -\frac{4z\mathscr{J}}{N\mu_0 g^2\mu_B^2}, \tag{17}$$

where $\mathscr{J}$ is the nearest neighbour exchange energy, N the number of sublattice atoms and z the number of nearest neighbours.

The magnitudes of M_A and M_B values can then be rearranged in terms of the Curie constant[2] as:

$$M_A + \frac{\lambda_N C}{2T}M_B = \frac{C}{2T}H \quad \text{and} \quad M_B + \frac{\lambda_N C}{2T}M_A = \frac{C}{2T}H, \tag{18}$$

and hence total magnetisation can be given by

$$M = M_A + M_B = \frac{C}{T + T_N}H, \tag{19}$$

which uses the notion of an antiferromagnetic Curie Temperature: a Néel Temperature, defined by $\mathrm{T}_N = \lambda_N\frac{C}{2}$. Above this temperature, thermal effects dominate; antiferromagnetic effects are no longer observed as the material begins to act as a paramagnet.

IV. METHODOLOGY

The Ising and Néel models are implemented using the programs "*ising*" and "*néel*" respectively, which are companions to the book "*Simulations for Solid State Physics*"[6]. The following is a brief description of how these programs implement the models.

A. The "ising" program

"*ising*" simulates the Ising model on a two dimensional grid, using a Monte-Carlo algorithm in which each spin is equilibrated with its four nearest neighbours according to Boltzmann distribution weighting factors. In "*ising*", values for the temperature T and magnetic field strength H are given in units of $\mathscr{J}$, where $\mathscr{J}$ is the interaction energy taken from equation (2). Thus $T = T_0$ means $k_B T_{\text{true}} = T_0\mathscr{J}$, with k_B the Boltzmann constant and T_{true} the true temperature. Similarly, $H = H_0$ means $\pm\mu H_{\text{true}} = \pm H_0\mathscr{J}$, with H_{true} the true magnetic field strength and μ a spin moment which corresponds to the interaction energy $\pm H_0\mathscr{J}$. M is also referred

to as the "magnetisation" of the grid, but is is in fact the normalised magnetisation $M = M_t/M_0$, where M_t is the true magnetisation and $M_0 = N\mu$ is the saturation magnetisation, obtained by aligning all of the N spins on the grid. From now on, when in reference to the Ising model, T, H and M are implicitly in units of $\mathscr{J}$. A spin in the Ising model is either assumed to be "up" or "down", so a spin S_i is 1 (up) or -1 (down). The energy of a spin S_i is

$$\mathcal{E}_i = -S_i\Big(\mathscr{J}\sum_{\langle j\rangle} S_j + H\Big) \equiv -S_i H_i^{\text{eff}}, \tag{20}$$

where the sum is over the four nearest neighbours of spin S_i. The probability of a spin pointing up at a temperature T is given by

$$p(S_i = 1) = \frac{e^{H_i^{\text{eff}}/T}}{e^{-H_i^{\text{eff}}/T} + e^{H_i^{\text{eff}}/T}}. \tag{21}$$

Subsequently, the probability of a spin pointing down is $p(S_i = -1) = 1 - p(S_i = 1)$. "*ising*" starts with a grid of predefined spins. It then randomly selects a spin S_i from the grid, and leaves it pointing up with probability $p(S_i = 1)$ and down with probability $p(S_i = -1)$. A single "sweep" consists of N of these processes, where N is the number of spins on the lattice. The number of sweeps that "*ising*" makes is decided by the user. "*ising*" uses periodic boundary conditions, meaning spins on an edge of the lattice counts spins on the opposite edge as neighbours.

B. The "néel" program

"*néel*" is an extension of "*ising*". It consists of a 30×60 lattice of spins, each of which interact with the external field, with their four nearest neighbours and also with every other spin in the lattice through dipole-dipole exchange. The temperature, T, magnetic field, H, dipole coupling constant, D and magnetisation M now dimensionless. For the cases considered in this paper, the energy of a spin S_i is

$$\mathcal{E}_i = -S_i\Big[\mathscr{J}\sum_{\langle j\rangle} S_j - D\sum_{j\neq i}\frac{a^2}{r_{ij}^2}S_j + H\Big] = -S_i H_i^{\text{eff}}. \tag{22}$$

In some antiferromagnetic lattices there is no single absolute ground state, a grid of odd numbered edges with periodic boundary conditions for instance. In a free boundary 30×60 grid, it is possible for all spins to be anti-parallel to their neighbours so this phenomenon (known as frustration), can be ignored. Free boundary means that at the edges, spins are considered to have no nearest neighbours that would lie outside of grid, or equivalently that $\mathscr{J} = 0$ for spins outside the grid.

V. RESULTS

A. Note on errors

For the plots in the following section, no error bars are shown. This is due to the high precision of the data from the simulations meaning that the error bars were too small to be clearly shown.

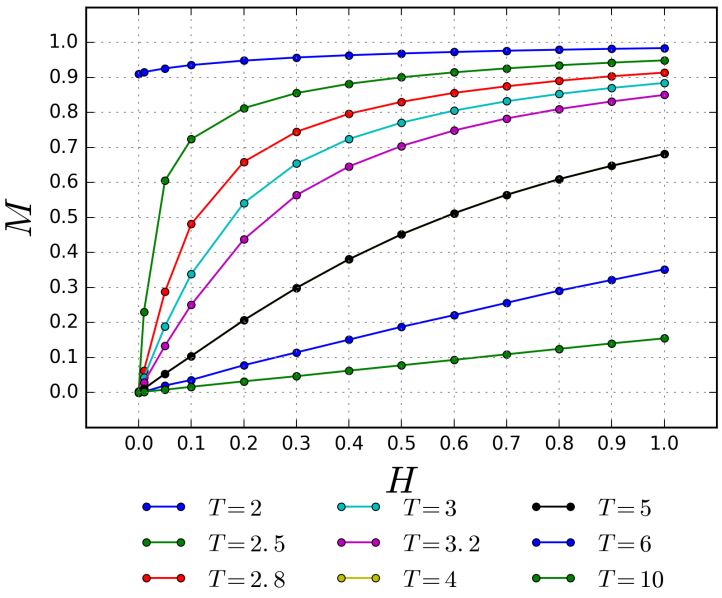

FIG. 1: Magnetisation, M, of a lattice of 100×100 spins in the "*ising*" program against magnetic field, H, at different temperatures. $T = 2$ shows spontaneous magnetisation at $H = 0$, expected for $T < T_C$. The other temperatures show $M = 0$ at $H = 0$, which is expected for $T \geq T_C$. For $T = 6, 10$, the trend is linear, so obeys the Curie-Weiss law, meaning $T \gg T_C$.

B. Magnetisation in the Ising model

The dependence of the magnetisation on external field of the Ising model at various constant temperatures was tested using the "*ising*" program. A lattice of 100×100 spins was used, with the same initial configuration for each run, which is a random grid with a low magnetisation value of $M = -0.0098$. Values for T in the range 1 to 10 were tested, with H taken between 0 and 1. For each H and T, the simulation was run for 10^4 sweeps and the final magnetisation recorded. This was repeated 10 times and an average taken to minimise error. FIG.1 shows the plot.

Below the Curie temperature, T_C, we expect there to be a spontaneous magnetisation in the absence of magnetic field. FIG.1 shows that this happens for $T = 2$, so we can conclude that $T_C > 2$. For all other temperatures plotted, $M \approx 0$ at $H = 0$, which is predicted to happen for $T \geq T_C$. For $T \gg T_C$, the Curie-Weiss law (equation (15)) is valid. In the units used by "*ising*", this is given in terms of the normalised susceptibility χ_n where

$$\chi_n \equiv \frac{M}{H} = \frac{1}{T - T_C}. \tag{23}$$

Thus equation (23) implies for fixed $T \gg T_C$, M is linearly proportional to H. This linear relationship is observed in FIG.1 for $T = 6, 10$, so we can conclude that $T_C < 6$.

C. Calculation of Curie temperature in the Ising model

For further study of the Ising model, a value for the Curie temperature, T_C, of the simulation was required. This was found using temperatures in the range $T = 6$ to 14, which is

known to be a region where the Curie-Weiss law (23) is valid (see section V B). For each value of T, H was fixed so that $M < 0.25$. Calculating a trend-line for $\frac{H}{M}$ against T for this data gives

$$\frac{H}{M} = (0.95 \pm 0.06)T - (3.09 \pm 0.04). \tag{24}$$

Comparison to equation (23) gives

$$T_C = 3.09 \pm 0.4. \tag{25}$$

$$k \in K \tag{26}$$

D. Dependence of magnetisation on temperature and magnetic field

1. "ising model"

Mean field theory predicts the magnetisation resulting from the Ising model is given by equation (6). Simulations of the Ising model were made to determine the accuracy of this approximation. Using the units used by "*ising*", equation (6) is written[6]

$$M = \tanh\left(\frac{H + 4M}{T}\right). \tag{27}$$

We define ΔM as a measure of the accuracy of equation (27), where

$$\Delta M(H, T, M) = \left| M - \tanh\left(\frac{H + 4M}{T}\right)\right|. \tag{28}$$

Note $\Delta M \in [0, 2)$ (as $M \in [-1, 1]$, $\tanh(a) \in (-1, 1) \forall a \in \mathbb{R}$), so we can say equation (27) is 100% accurate at a point where $\Delta M = 0$, and 0% accurate when $\Delta M = 2$. A lattice of 100×100 spins was used, with $H \in [0.1, 1.0]$, increasing in increments of 0.1. The lattice was initialised with the same initial conditions as in section V B each run. Each simulation was run for 10^4 sweeps, and the final M recorded. T was started at 0.1 and gradually increased until the $M < 0.1$, at which point there are approximately the same number of spins up as there are down. FIG. 2 shows graphs of ΔM against T for the differing values of H.

Recall $T_C = 3.09 \pm 0.04$, from equation (25). FIG. 2a shows that there are sharp peaks in ΔM near the Curie temperature, the highest value being $\Delta M = 0.1306 \pm 0.0003$ for $H = 0.1$ at $T = 2.6$, which is an accuracy of $(93.47 \pm 0.02)\%$. This peak decreases as H increases, until $H = 0.7$ where there is no longer a peak near T_C. Instead, as seen in FIG.2b, a softer peak appears at $T = 6$. Unlike the first peak, this uniformly increases as H increases, up to a maximum of $\Delta M = 0.1063 \pm 0.0005$ for $H = 1.0$, an accuracy of $(94.68 \pm 0.03)\%$. Note this still may increase if higher values of H were tested.

2. "néel" model

A similar study can be conducted in the Néel model. Again we use the same random initial condition for each measurement, but this time with an initial M value of $M = 0$, and on a 30×60 grid. However, we lack a similar analogue to the total

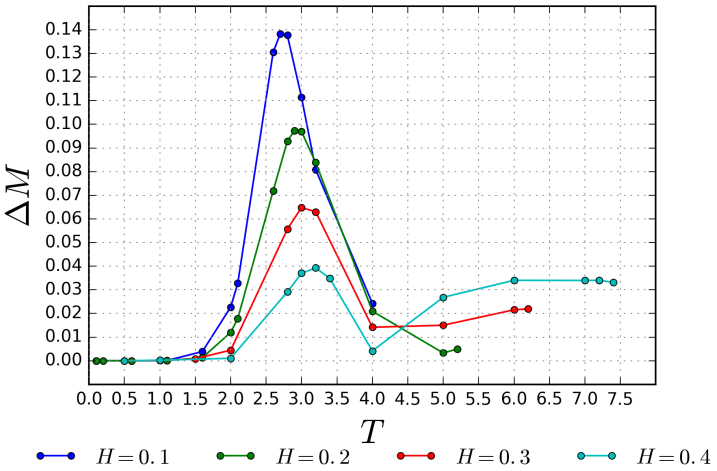

(a) $H < 0.5$

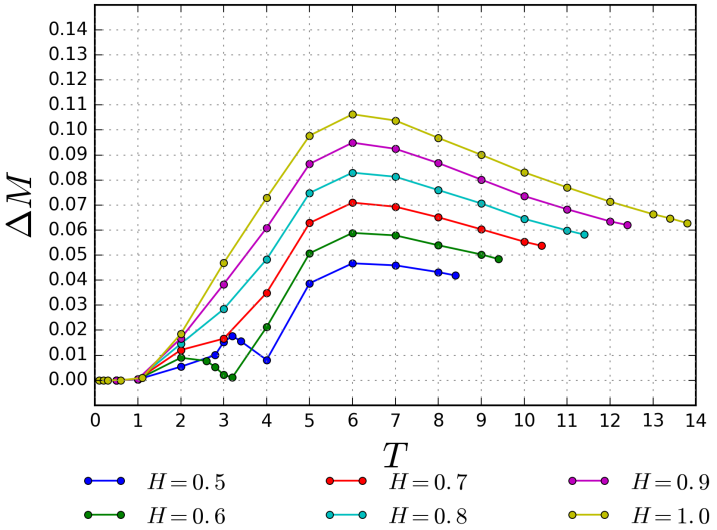

(b) $H \geq 0.5$

FIG. 2: Plots of ΔM against T for values of H from 0.1 to 1.0. FIG. 2a shows lines for $H < 0.5$, where the peak value for ΔM for each H is near $T = 3$. FIG. 2b shows lines for $H \geq 0.5$, where the peak value for ΔM shifts to around $T = 6$. The plots for each series stop once M becomes less than zero, hence smaller H values have shorter ranges.

magnetisation equation given for the Ising model (6). We can formulate spontaneous magnetisation equations for each sublattice, but these are irrelevant as the Néel model predicts that below the Néel temperature, $\mathbf{M}_A$ = -$\mathbf{M}_B$, and hence $\mathbf{M}$=0. Far above the Néel temperature though, the Curie-Weiss Law is again expected to be followed, but this time in a modified state seen in equation (19). To investigate the region between these known regimes, we look at the magnetic susceptibility of the model. This is defined as $\chi = \frac{M}{H}$, and our value is taken as an average of $\frac{M}{H}$ over each of the H values measured in FIG. 2a and FIG. 2b, and is plotted in FIG. 3.

As T approaches 0 we see that magnetic susceptibility also approaches 0. This is expected in our model as our "easy axis" is parallel to the external magnetic field. At $T = 0$ there are no thermal fluctuations, so the angle between spin and field is always 0° or 180°. This means that given any arbitrarily large H, the magnetic energy is at a maximum for

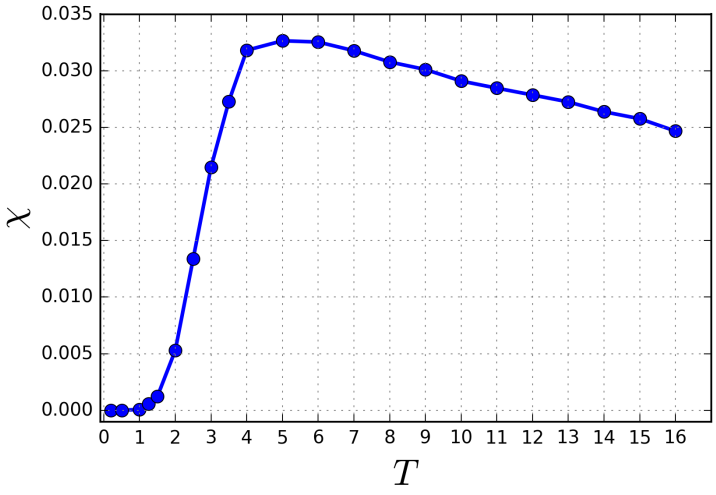

FIG. 3: Plot of temperature against magnetic susceptibility for values of χ averaged over multiple H values. Notice the intercept at the origin and the change in shape around $T = 4$

the aligned spin and at a minimum for the anti-aligned spin. Due to the lack of thermal fluctuations there is no energetically direction in which to rotate the anti-aligned spin, so by the simple argument of symmetry; it does not rotate. This means that the magnetisation is 0 for all H at $T = 0$. Now observing the behaviour around $T = 4.5$ we see that the initial increasing region shifts into a smoother decreasing regime. This critical point is expected as the "*néel*" simulation has a T_N value of $4\mathscr{J}$. Although we have derived no analytical prediction to compare this with, the increasing region matches observations of real antiferromagnetic materials like ferritin[7]. After this curve change, we see a gradual decrease. According to the modified Curie-Weiss Law (19), we should see a $\chi \approx \frac{C}{T+T_N}$ pattern here as temperature increases. However, this is clearly not the case between $T = 4$ and $T = 8$, but this is conceivably due to T being too close to T_N; after $T = 10$ it is feasible that the predicted pattern would line up with the slight decline in the plot.

E. Magnetisation reversal times of the Ising model below the Curie temperature

Considering a 25×25 spin lattice in "*ising*", whose spins were initially all positive (giving mean magnetisation, $\langle M \rangle = 1$), in the presence of external magnetic fields, $H \in \{-0.5, -1.0, -1.5\}$. The mean number of sweeps taken for $\langle M \rangle$ to cross 0 at varying magnetic field and temperatures below T_C was measured. The simulation showed that the number of sweeps taken for spin reversal decreases with both increasing temperature and field magnitude, the former due to the increased influence of thermal fluctuations, and the latter due to the external field giving a preferential magnetisation to the system. Using the simulation and equation (21) enabled us to determine the following relation

$$t(t_0) = \exp\left(\frac{1}{\alpha T}\right), \tag{29}$$

where t is the number of sweeps taken to reach $\langle M \rangle = 0$, T is the temperature in terms of $\mathscr{J}$ and α is a coefficient which is approximately linearly proportional to the magnitude of the external magnetic field. This is illustrated in FIG. 4.

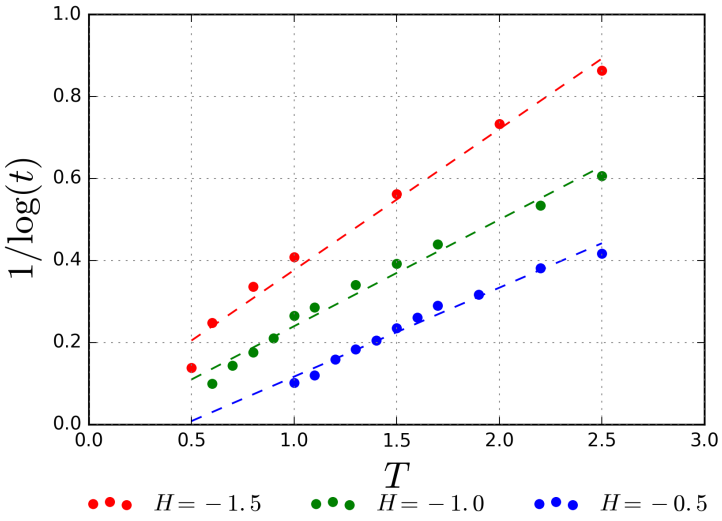

FIG. 4: Plot of $\frac{1}{log(t)}$ against T for values of H from -0.5 to -1.5.

The relationship was approximately determined to be

$$\alpha = (-0.13 \pm 0.05)H + 0.15 \pm 0.02, \tag{30}$$

where H is the magnitude of the external magnetic field. At low temperatures the number of sweeps necessary became too large to be able to feasibly record.

In running the simulation it was possible to observe how magnetisation reversal was affected by nucleation as small areas of aligned spins would spontaneously form small areas or 'grains' of aligned spin. If these grains had a magnetisation opposite to the applied field, an individual spin neighbouring a grain would be more likely to flip to be parallel with its neighbours, rather than to be parallel with the applied field. However, these grains of opposite spins were very unlikely to grow large enough that the overall system inverts in magnetisation, becoming antiparallel to the applied field as the effect of thermal fluctuations below the Curie temperature is very small so this was never observed.

VI. DISCUSSION

For the magnetisation of the Ising model in section V B simulations were in agreement with the mean field theory prediction at $H = 0$ for $T = 2$ and $T \geq 3.2$. However for the measured value of $T_C = 3.09 \pm 0.04$, it was expected that for $T = 2.5$, 2.8 and 3.0 (below T_C), their magnetisation would be non-zero at $H = 0$, which was not observed. This discrepancy could be attributed to an error in the measured value of T_C. The shape of the plot agrees well with experimental data for ferromagnetic materials, as seen in Fig. 4 of[8]. The mean field theory predicts $T_C = 2$, so there is a large discrepancy from the measured value of T_C. A possible cause of this would be an instability in the estimate for T_C. T_C is defined by Curie-Weiss law, but this is only valid for $T \gg T_C$, hence the data points taken in section V C were far from the origin, meaning small errors in these measured values cause large deviations in the intercept of the trend-line, which was used to calculate T_C. Section V D 1 shows that equation (6), derived from mean field

theory, is a good estimate for the magnetisation in the ranges of H and T measured, with a minimum accuracy of 93.45%.

For the magnetisation of the Néel model in section **??**, low temperature simulations were more in agreement with experimental results than the Ising model. T_N was found to be almost exactly at the value predicted by the Néel model, $T_N = 4$, as shown by the sudden curve change in FIG. (3. The simulation also correctly showed an intercept at 0, despite the potential for a possible $\frac{0}{0}$ divergence error, and showed an experimentally verified[7] relationship for $T \in [0, T_N]$. Above T_N, the model began to fail, presumably because it focuses on antiferromagnetic properties which disappear after T_N. The modified Curie-Weiss Law (19) predicted by mean field theory was not seen directly above T_N, the main shortcoming of the "*néel*" simulation. However, as T increased far above T_N the Law was eventually matched ($T > 13$). By contrast, the original Curie-Weiss Law (23) for the Ising model was matched after $T = 6$.

The investigation into magnetisation reversal times under the Ising model showed that the model predicts that a system will eventually undergo total magnetisation reversal when an external magnetic field is applied. Using this model, the system was never observed to adopt an average magnetisation opposite to the applied field when run below the Curie temperature, showing that thermal fluctuations at this temperature are rarely enough to create a nucleus large enough to gain control over the entire system. Reducing the magnitude of the external field led to longer reversal times as the grains caused by the nucleation process were able to become larger before decaying. Likewise, lower temperatures led to longer reversal times as the mean field theory predicts an exponential dependence on $\frac{1}{T}^2$ which was demonstrated by our model and also displayed here[9]. It is notable that this exponential dependence on the inverse temperature exhibited by the model differs from that of real ferromagnets which display a $\frac{3}{2}$ power law dependence, this is because the Ising model fails to account for the contributions of transverse components of the spin[2]. Ising also fails to account for the dipole-dipole interactions considered under the Néel model. These interactions mean that nucleation does not occur as each particle interacts ferromagnetically with some neighbours and antiferromagnetically with others. Instead, the dipole-dipole interaction causes domains to form within the structure and the magnetisation now responds reversibly to the applied field so total magnetisation reversal is not observed.

VII. CONCLUSION

The investigation determined that the "*ising*" simulation accurately reflects the expected behaviour from the mean field theory, but fails to precisely locate the Curie Temperature. The "*néel*" simulation accurately reflects experimental behaviour up to and at T_N but largely fails to reflect the subsequent paramagnetic phase predicted by the mean field theory. It would be pertinent to continue this investigation of magnetism simulations by increasing the grid dimensions in both simulations to quantify the effect of the boundary conditions on our observations. The "*ising*" simulation could be subjected to higher fields so as to determine whether the increasing ΔM values in FIG. 2b ever stabilise. It would also be worth introducing periodic or constant boundary conditions for the "*néel*" simulation, which would induce geometrical frustration to the grid.

VIII. REFERENCES

[1] M. Weisheit, S. Fähler, A. Marty, Y. Souche, C. Poinsignon, and D. Givord, "Electric field-induced modification of magnetism in thin-film ferromagnets," Science **315**, 349–351 (2007).

[2] H. E. Hall, and J. R. Hook, *Solid State Physics*, 2nd ed. (Wiley, 2013).

[3] Computational Physics Group, Technion, "Derivation of the Heisenberg Hamiltonian for The Hydrogen Molecule," `http://phycomp.technion.ac.il/~riki/H2_molecule.html`, [Online; accessed 02-03-2017].

[4] J. Selinger, *Introduction to the Theory of Soft Matter From Ideal Gases to Liquid Crystals* (Springer, 2016).

[5] Richard Fitzpatrick, Nikos Drakos, Ross Moore, "The Ising Model," (2006).

[6] R. H. Silsbee, and J. Dräger, *Simulations for Solid State Physics* (Cambridge University Press, 1997).

[7] N. J. O. Silva, A. Millán, F. Palacio, E. Kampert, U. Zeitler, H. Rakoto, and V. S. Amaral, "Temperature dependence of antiferromagnetic susceptibility in ferritin," Phys. Rev. B **79**, 104405 (2009).

[8] M. Toprak, H. Kavas, Y. Koseoglu, and B. Aktas, "Synthesis of Fe3O4 nanoparticles at 100 C and its magnetic characterization," Journal of Alloys and Compounds **472** (2009), 10.1016/j.jallcom.2008.04.101.

[9] K. Brendel, G. T. Barkema, and H. van Beijeren, "Magnetization reversal times in the two-dimensional ising model," Phys. Rev. E **67**, 026119 (2003).